

⁵ Schmidt, E. M. and Cresci, R. J., "Near Wake of a Slender Cone in Hypersonic Flow," *AGARD Fluid Physics of Hypersonic Wakes*, Vol. 1, May 1967, pp. 1-31.

⁶ Murphy, J. R., "Initial Operation and Calibration of the UMR Supersonic Axisymmetric Wind Tunnel," MS thesis, 1970, Mechanical and Aerospace Engineering Dept., University of Missouri—Rolla, Rolla, Mo.

⁷ Mirly, K. A., "Experimental Studies of Supporting Wire Disturbances in the Near Viscous Wakes of Slender Bodies," MS thesis, 1972, Mechanical and Aerospace Engineering Dept., University of Missouri—Rolla, Rolla, Mo.

⁸ McLaughlin, D. K., Carter, J. E., and Finston, M., "Experimental Investigation of the Near Wakes of a Magnetically Suspended Cone at $M = 4.3$," AIAA Paper 69-186, New York, 1969.

Scaling of Performance and Thermal Environment in Fuel-Vortex Cooled Rocket Engines

K. BERMAN,* T. FERGER†
N. ROTH‡ AND A. BLESSING§
Bell Aerospace Company, Buffalo, N. Y.

Nomenclature

A, B, C, D, N	= experimentally determined constants
A_t	= throat area, in. ²
c^*	= over-all characteristic velocity, fps
c_c^*	= core characteristic velocity, fps
c_b^*	= barrier characteristic velocity, fps
D_c	= cylindrical chamber diameter, in.
L	= axial length of engine from vortex lip to throat, in.
P_c	= chamber pressure, psia
r_o	= over-all mixture ratio
r_c	= core mixture ratio
T_{max}	= maximum wall temperature at zero heat transfer, °F
ρ	= barrier coolant flow/total propellant flow
h_c	= heat-transfer coefficient from core to barrier, BTU/ft ² -hr °F
h_g	= heat-transfer coefficient from barrier to wall, BTU/ft ² -hr °F
\dot{W}_c	= film coolant flow rate, lb/sec
\dot{W}_t	= total flow rate, lb/sec
\dot{Q}	= heat rejection rate to barrier by core, BTU/sec
\dot{q}	= heat flux, BTU/in. ² -sec
ΔT	= average temperature gradient between core and coolant, °F
$C_{F\infty}$	= thrust coefficient for expansion to vacuum
η	= combustion efficiency

Introduction

IN a previous communication,¹ results of various barrier cooling concept evaluations were presented. It was observed that the vortex barrier cooling technique did provide an extremely uniform wall thermal environment at controllable and predictable values. In this Note additional investigations are reported with the fuel-vortex barrier concept. Nitrogen tetroxide (N_2O_4) was the oxidizer employed and monomethyl

hydrazine (MMH) or 50% hydrazine-50% unsymmetrical dimethyl hydrazine (A-50) were used as respective fuel components. The range of the investigations covered thrust levels from 400 to 5500 lb and chamber pressure ranges from 100 to 300 psia. Within the range of variables investigated, correlations were established which allow prediction of the amount of barrier flow required to obtain a maximum desired wall temperature, having given the chamber geometry and operating conditions. A cross-correlation between performance and the maximum wall temperature was also established.

Thermal environment

The investigations reported in Ref. 1 indicated that the fuel-vortex barrier technique possesses the potential to attain these technical objectives. Therefore, the scope of the investigations was expanded to make a systematic evaluation of pertinent parameters. Among these were included the effects of various amounts of barrier flow, effect of primary core pattern, mixture ratio and chamber pressure. The initial test series was again conducted with a modular type injector (Fig. 1), consisting of a separately fed core of triplet and doublet elements and a separately fed barrier. However, the stainless steel chamber was replaced by a 3.4-in.-diam radiation-cooled, coated columbium chamber. This allowed the use of multiple Pyroscanners to obtain a thermal profile of the engine continuously during the test. This permitted a direct measurement of temperature uniformity and maximum wall temperature as well as the definition of the wall temperature transient through equilibrium, usually about 30 sec. As explained in Ref. 1, from the latter data, it is possible to compute the effective gas-side heat-transfer coefficients and wall driving temperature by assuming one-dimensional radial heat flow. Since the heat balance requires that at any instant the heat input to the wall from the combustion gas is equal to the sensible heat absorbed by the wall plus the radiant heat lost to the environment, a plot of \dot{q} vs wall temperature yields a line, the slope of which is the value of the "effective" gas-side heat-transfer coefficient, and the intercept of which represents the local gas-driving temperature. To confirm the values of the gas-driving temperature thus computed, as part of an altitude cell test series with the same hardware configuration, the engine was operated completely insulated. Wall temperatures were measured by means of imbedded thermocouples in these tests. The agreement between the driving gas temperatures measured by these two techniques was very good. Since the specific impulse and/or characteristic velocity were measured simultaneously, a direct correlation between performance and thermal profile became readily available.

The Pyroscanner data confirmed the previous observation that the temperature uniformity produced by the vortex sheet is very good. This is illustrated by a typical Pyroscanner printout shown in Fig. 2. It shows the temperature profile

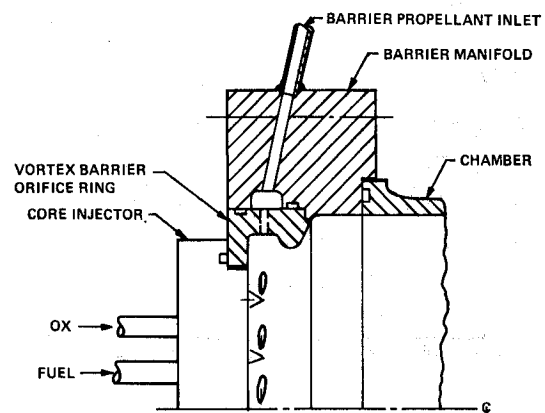


Fig. 1 Vortex barrier injector schematic.

Presented as Paper 72-1075 at the AIAA/SAE 8th Joint Propulsion Specialist Conference, New Orleans, La., November 29-December 1, 1972; submitted December 8, 1972; revision received March 23, 1973.

Index categories: Liquid Rocket Engines; Boundary Layers and Convective Heat Transfer—Turbulent.

*Chief Engineer, Development and Technology.

†Research Scientist.

‡Chief, Bipropellant Combustion Devices.

§Chief, Heat Transfer.

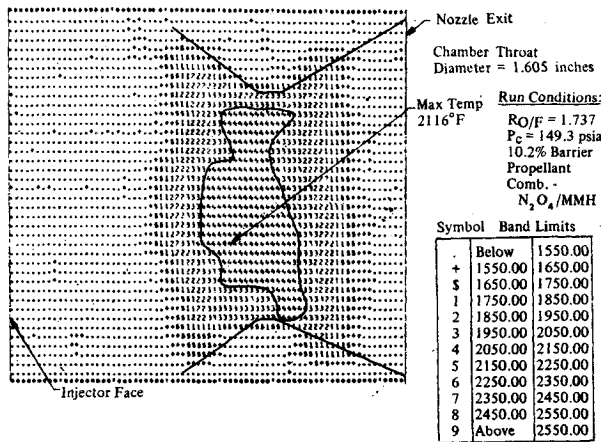


Fig. 2 Pyroscanner plot.

after steady-state conditions have been achieved. It indicates that the temperature distribution in any cross-section increases axially in a monotonic manner towards a maximum value upstream of the throat and then decreases in the same fashion downstream. At any given cross-section, it appears as if there exists a decrease in temperature as the 12 and 6 o'clock chamber surfaces are approached. This, however, is a function of the Pyroscanner orientation, since the view factor and exact engine silhouette are very difficult to define precisely at the "horizons."

For a given configuration, the maximum wall temperature, which generally occurs near the throat, is a function primarily of the ratio of barrier flow to total propellant flow, ρ . A statistical multiple-regression analysis of the 3.4-in.-diam engine thermal data was employed to assess the significance of the various operating parameters on the maximum steady-state wall temperature, i.e.,

$$T_{\max} = A\rho + B(r_o) + C(P_c) + N \quad (1)$$

It was found that over the range of parameters investigated, i.e., $0.08 < \rho < 0.14$; $125 < P_c < 300$; $1.4 < r_o < 1.8$, ρ is the only significant parameter and the data for a given geometric configuration are correlated well by a relationship

$$\rho = (N' - T_{\max})/A \quad (2)$$

where N' is a constant which includes the average influence of r_o and P_c .

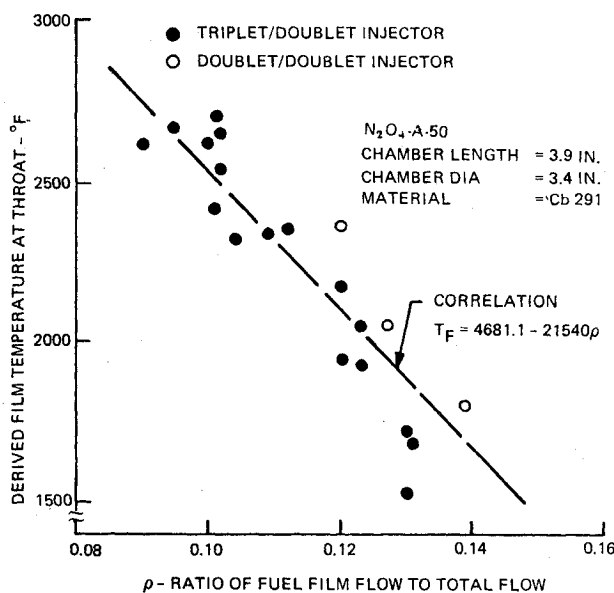


Fig. 3 Film temperature at throat vs film flow ratio.

Figure 3 is a plot of T_{\max} vs ρ for A-50 as the barrier coolant. The data include tests from the Pyroscanner as well as the completely insulated test series. Good correlation is indicated. Obviously the relationship will not remain linear as ρ becomes larger, since the driving temperature must become asymptotic to the decomposition temperature of the fuel coolant. For this specific configuration, having a $D_c = 3.4$ in., $L = 3.9$ in., $D_t = 1.605$ in., Eq. (2) becomes

$$\text{for A-50: } \rho = (4681 - T_{\max})/21540 \quad (3)$$

$$\text{for MMH: } \rho = (4381 - T_{\max})/21540 \quad (4)$$

The approximate computed local heat transfer coefficients at the highest temperature locations, normalized to 150 psia chamber pressure, are

$$\text{For A-50 coolant: } h_g = 700 \text{ BTU/hr-ft}^2 \text{ } ^\circ\text{F}$$

$$\text{For MMH coolant: } h_g = 1040 \text{ BTU/hr-ft}^2 \text{ } ^\circ\text{F}$$

Indications have been that the primary core pattern was not a significant parameter in influencing the barrier flow requirements. In order to assess this more thoroughly, an injector core consisting of 36 doublet elements was fabricated and tested in addition to the existing triplet/doublet pattern. Although this injector produced a large increase in performance (about 100 fps Δc^*), no significant deviation in the T_{\max} vs ρ correlation can be determined.

To evaluate the effect of combustor geometry and thrust on the relationship between T_{\max} and ρ , an integrated analytical and experimental program was undertaken. The basic hypothesis underlying the analytical model is that the ratio of film coolant flow rate (\dot{W}_c) to heat rejected (\dot{Q}) to the barrier, as it moves from the point of injection to the throat, is a constant if the identical maximum film temperature is to be reached. Thus, for two engines to have the same maximum film temperature, the barrier flow rate would have to be proportional to the heat rejected, i.e.,

$$\dot{W}_{c1}/\dot{W}_{c2} = \dot{Q}_1/\dot{Q}_2 \quad (5)$$

The total heat rejected to the barrier is approximated by

$$\dot{Q} = \pi D_c h_c L \Delta T \quad (6a)$$

and the following substitutions are made in Eq. (5)

$$\dot{W}_c = \rho \dot{W}_t$$

$$h_c = D(1/D_c^{1.8})(\dot{W}_t)^{0.8} \quad (6b)$$

$$\dot{W}_t = g P_c A_t / c^*$$

Assuming that $\Delta T_1 = \Delta T_2$ to reach the same maximum wall temperature, Eq. (5) becomes

$$\rho_1/\rho_2 = (L_1/L_2)(D_2/D_1)^{0.8} \frac{(c_1^*/P_{c1}A_{t1})^{0.2}}{(c_2^*/P_{c2}A_{t2})^{0.2}} \quad (7)$$

Substituting the data gathered with the 3.4-in.-diam engine, i.e., Eq. (3), the A-50 barrier flow rate ρ required to establish a desired maximum insulated wall temperature is

$$\rho = [(4848 - T_{\max})/58085][L/D_c^{0.8}](c^*/P_c A_t)^{0.2} \quad (8)$$

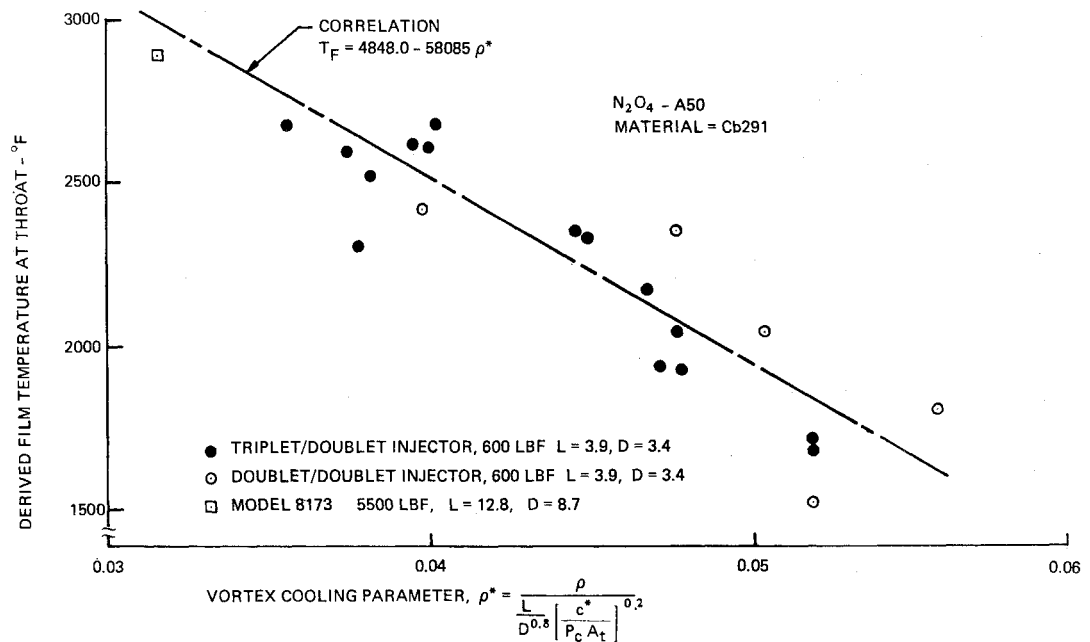
A similar equation can be written for MMH coolant.

To confirm the validity of such a scaling correlation, tests have been conducted so far with the configurations shown in Table 1. In Fig. 4, the maximum wall temperatures derived

Table 1 Configuration tested for ρ^* correlation

Nominal thrust, lb	\bar{L} in.	D_c in.	L^* in.	D_t in.
500	3.9	3.4	14	1.605
500	5.0	3.4	20.2	1.605
600	3.6	3.4	14	1.451
600	4.0	3.4	16.3	1.451
5500	12.8	8.7	26	6.103
3500	10.0	8.0	31	4.578

Fig. 4 Film temperature at throat vs vortex film parameters.



from these tests have been plotted, based on Eq. (8) vs the cooling parameter $e^* = e / [(L/D^{0.8})(c^*/P_c A_t)^{0.2}]$. The experimental data confirms that within the range of parameters investigated, this model provides a satisfactory correlation and scaling method.

Performance

The performance achieved is, of course, a function of the injector design and engine geometry. If the overall characteristic velocity is written as the weight-averaged linear combination of the primary core and barrier performance, the expected overall c^* is

$$c^* = \eta c_c^* - (\eta c_c^* - c_b^*)\rho \quad (9)$$

where c_c^* is the theoretical core characteristic velocity at its operating mixture ratio and η is the combustion efficiency. In view of its definition, the variable ρ is related to the core and over-all mixture ratios as follows

$$\rho = (r_c - r_o)/r_c(1 + r_o) \quad (10)$$

The core mixture ratio for $1.4 < r_o < 1.8$ will be somewhat near 2.0. At the higher mixture ratios c_c^* for the propellant combination A-50/ N_2O_4 is nearly linear with r_c and can be approximated by the expression

$$c_c^* = 5650 + [2.0 - r_c](350) \quad (11)$$

Substituting Eqs. (10) and (11) into Eq. (9), one obtains

$$c^* = 6350\eta - \frac{(1-\rho)(350)\eta}{(1-\rho-\rho r_o)} r_o - (\eta 6350 - c_b^*)\rho \quad (12)$$

For small variations in ρ the coefficient of r_o is nearly constant with the result that Eq. (12) has essentially the same form as that derived from the multiple regression analysis of the performance data plotted in Fig. 5.

The importance of the primary core efficiency on over-all performance is shown by these data, where the use of the doublet configuration produced an increase of about 100 fps in characteristic velocity. The data points can be correlated by the following relations within the range $1.4 < r_o < 1.8$. For the triplet/doublet core (N_2O_4 - A-50):

$$c^* = 6708 - 646r_o - 4475\rho \quad (13)$$

For the doublet core (N_2O_4 - A-50):

$$c^* = 6752 - 604r_o - 3464\rho$$

The measured $C_{F\infty}$ with N_2O_4 - A-50 for a 25.3:1 area ratio nozzle at $r_o = 1.6$ averaged about 1.738. This value compared

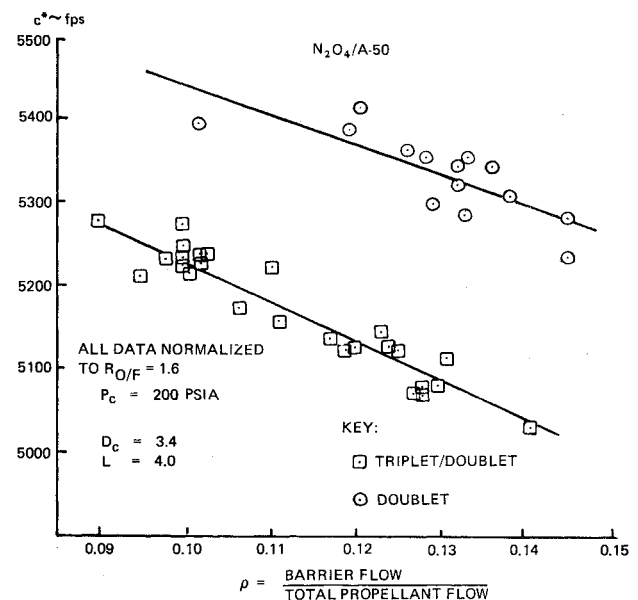


Fig. 5 Correlation of c^* vs percentage barrier flow.

well with the predicted values using the two-dimensional kinetics computer program and making appropriate corrections for boundary-layer losses.

Performance/temperature tradeoff

It is apparent that for a selected T_{max} , the magnitude of ρ is primarily a function of the engine geometry, i.e., the length L and the chamber diameter D_c . The performance of a given injector, on the other hand, is primarily a function of the basic combustion efficiency of the injector primary core pattern, the associated geometric dimensions (L^*) of the engine and the value ρ . Once the c^* variations are established as a function of L and D_c , it is possible therefore to compute the minimum ρ value required to obtain maximum performance for the selected maximum wall temperature

Reference

- Berman, K. and Andrysiak, S. J., "Barrier Film Cooling Study," *Journal of Spacecraft and Rockets*, Vol. 9, No. 3, March 1972, p. 152.